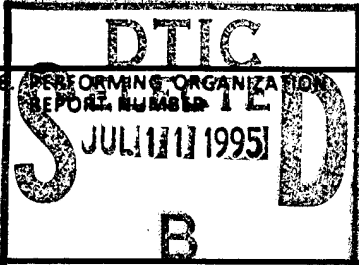


# REPORT DOCUMENTATION PAGE

Form Approved

OMB No. 0704-0188

Public reporting burden for this collection of information is estimated to average 1 hour per response, including the time for reviewing instructions, searching existing data sources, gathering and maintaining the data needed, and completing and reviewing this collection of information. Send comments regarding this burden estimate or any other aspect of this collection of information, including suggestions for reducing this burden, to Washington Headquarters Services, Directorate for Information Operations and Reports, 1215 Jefferson Davis Highway, Suite 1204, Arlington, VA 22202-4302, and to the Office of Management and Budget, Paperwork Reduction Project (0704-0188), Washington, DC 20503.

|   |  |   |   |  |
|---|--|---|---|--|
| 1. AGENCY USE ONLY (Leave blank)  |  | 2. REPORT DATE<br>20 May 1995                           | 3. REPORT TYPE AND DATES COVERED<br>Final Report 3/20/1992 - 3/19/1995              |  |
| 4. TITLE AND SUBTITLE<br>Spectroscopic Study of Reaction Intermediates and Mechanisms in Nitramine Decomposition and Combustion   |  |   | 5. FUNDING NUMBERS<br><br>ARO MIPR 107-94   |  |
| 6. AUTHOR(S)<br><br>Marilyn E. Jacox  |  |   |  |  |
| 7. PERFORMING ORGANIZATION NAME(S) AND ADDRESS(ES)<br><br>Molecular Physics Division<br>National Institute of Standards and Technology<br>Gaithersburg, Maryland 20899  |  |   |   |  |
| 9. SPONSORING/MONITORING AGENCY NAME(S) AND ADDRESS(ES)<br><br>U. S. Army Research Office<br>P. O. Box 12211<br>Research Triangle Park, NC 27709-2211   |  |   | 10. SPONSORING/MONITORING AGENCY REPORT NUMBER<br><br>ARO 30094.5-CH                |  |
| 11. SUPPLEMENTARY NOTES<br>The view, opinions and/or findings contained in this report are those of the author(s) and should not be construed as an official Department of the Army position, policy, or decision, unless so designated by other documentation.   |  |   |   |  |
| 12a. DISTRIBUTION/AVAILABILITY STATEMENT<br><br>Approved for public release; distribution unlimited.  |  |   | 12b. DISTRIBUTION CODE  |  |
| 13. ABSTRACT (Maximum 200 words)<br><br>The infrared spectra of reaction intermediates trapped in solid neon were studied in order to support the development of diagnostics for short-lived species which are reaction carriers in nitramine decomposition and combustion and to derive information about reactions which are important in the condensed-phase decomposition of nitramines. Nitromethane and monomethylnitramine were used as model compounds in these studies. Evidence was obtained for the formation of water complexes with both of these species. The results support the water-catalyzed decomposition mechanism for nitramines that was proposed by Melius. Studies of the photodecomposition of isotopically substituted monomethylnitramine demonstrate that four different groups of products are formed. Tentative spectral assignments are made for the aci- isomer of monomethylnitramine and for CH <sub>3</sub> NHONO. The final photodecomposition products are CH <sub>4</sub> , NO, CH <sub>3</sub> OH, and N <sub>2</sub> O. Other studies have provided evidence for the formation of a weakly bonded complex of H <sub>2</sub> with H <sub>2</sub> O, as well as spectral data for the HCC free radical and for the H <sub>2</sub> O <sup>+</sup> , NO <sub>2</sub> <sup>+</sup> , NO <sub>2</sub> <sup>-</sup> , and NO <sub>3</sub> <sup>-</sup> molecular ions.<br><br>INFO QUALITY IMPROVED 3 |  |   |   |  |
| 14. SUBJECT TERMS<br>HCC; infrared spectrum; matrix isolation; molecular ions; CH <sub>3</sub> NHNO <sub>2</sub> ; near-infrared spectrum; CH <sub>3</sub> NO <sub>2</sub> ; photodecomposition; water complex; water-catalyzed nitramine decomposition   |  |   | 15. NUMBER OF PAGES<br>37   |  |
|   |  |   | 16. PRICE CODE  |  |
| 17. SECURITY CLASSIFICATION OF REPORT<br>UNCLASSIFIED   | 18. SECURITY CLASSIFICATION OF THIS PAGE<br>UNCLASSIFIED | 19. SECURITY CLASSIFICATION OF ABSTRACT<br>UNCLASSIFIED | 20. LIMITATION OF ABSTRACT<br>UL  |  |

**SPECTROSCOPIC STUDY OF REACTION INTERMEDIATES AND MECHANISMS  
IN NITRAMINE DECOMPOSITION AND COMBUSTION**

Final Report

Marilyn E. Jacox

20 May 1995

U. S. Army Research Office

Proposal 30094-CH

Molecular Physics Division  
National Institute of Standards and Technology  
Gaithersburg, Maryland 20899

Approved for public release;  
distribution unlimited.

19950703 301

The view, opinions, and/or findings contained in this report are those of the author and should not be construed as an official Department of the Army position, policy, or decision, unless so designated by other documentation.

|                      |  |
|----------------------|--|
| <b>Accession For</b> |  |
| NTIS GNA&I           | <input checked="checked" type="checkbox"/> |
| DTIC TAB             | <input type="checkbox"/>                   |
| Unannounced          | <input type="checkbox"/>                   |
| Justification        |  |
| By _____             |  |
| Distribution/        |  |
| Availability Codes   |  |
| Dist                 | Avail and/or<br>Special                    |
| A-1                  |  |

## Table of Contents

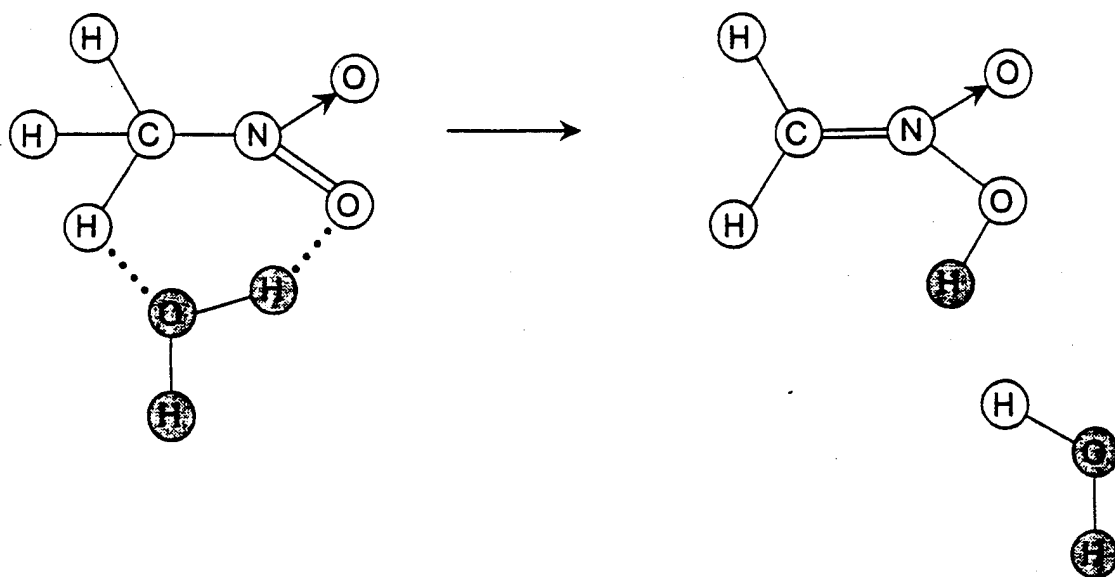
|  |    |
|--|----|
| Scientific Objectives  | 2  |
| Scientific Background  | 2  |
| Scientific Accomplishments   | 8  |
| Infrared Spectrum of H <sub>2</sub> O Trapped in Solid Neon                                    | 8  |
| Interaction of Nitro Compounds with H <sub>2</sub> O   | 8  |
| CH <sub>3</sub> NO <sub>2</sub>  | 8  |
| CH <sub>3</sub> NHNO <sub>2</sub>  | 12 |
| Photodecomposition of CH <sub>3</sub> NHNO <sub>2</sub>  | 16 |
| Other Studies  | 31 |
| Interaction Between H <sub>2</sub> O and H <sub>2</sub>  | 31 |
| Reaction of CH <sub>3</sub> NO <sub>2</sub> with H Atoms                                       | 31 |
| Infrared and Near Infrared Spectra of HCC and DCC  | 31 |
| Molecular Ions   | 33 |
| H <sub>2</sub> O <sup>+</sup>  | 33 |
| NO <sub>2</sub> <sup>+</sup> , NO <sub>2</sub> <sup>-</sup> , and NO <sub>3</sub> <sup>-</sup> | 34 |
| Search for Ions Derived from CH <sub>3</sub> NO <sub>2</sub>                                   | 34 |
| Publications   | 35 |
| Participants in ARO Research   | 35 |
| References   | 36 |

## Scientific Objectives

The focus of this project was on the conduct of experimental studies to provide spectroscopic data for reaction intermediates which are expected to play key roles in the decomposition and combustion of the nitramines, in order to obtain information on the nature of the detailed reaction mechanism and to facilitate the development of *in situ* probes for the reaction intermediates. One of the most important tasks of this research was to test the proposal by Melius<sup>1,2</sup> that water catalysis plays a significant role in the decomposition of nitro-aliphatic compounds and nitramines. An effort was also made to determine the nature of the processes which are important in the photodecomposition of monomethylnitramine, a prototype of more complicated nitramines such as RDX and HMX.

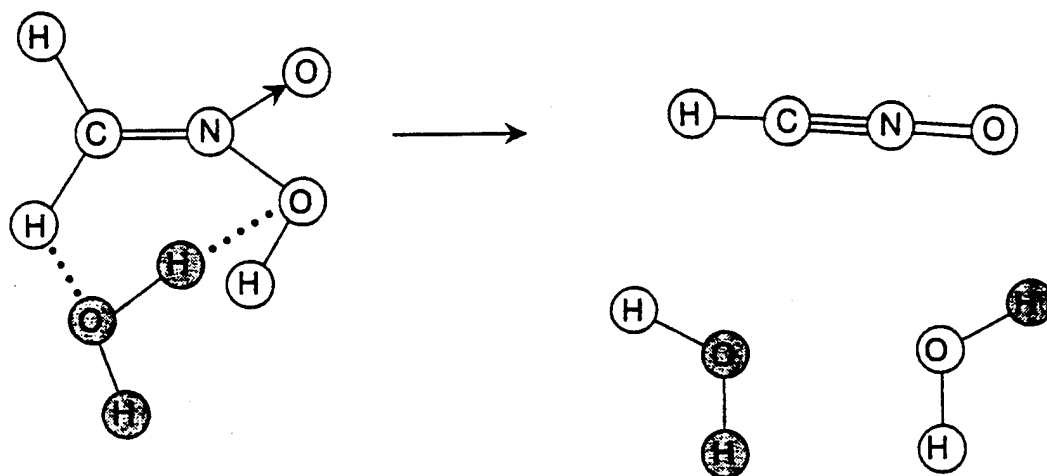
## Scientific Background

In both the calculations of Melius and the present experimental study, nitromethane ( $\text{CH}_3\text{NO}_2$ ) and monomethylnitramine ( $\text{CH}_3\text{NHNO}_2$ ) were used as model compounds. Melius<sup>1,2</sup> found that the interaction of  $\text{H}_2\text{O}$  with  $\text{CH}_3\text{NO}_2$  greatly reduces the barrier to the isomerization of  $\text{CH}_3\text{NO}_2$  to its *aci*- isomer,  $\text{CH}_2\text{N}(\text{O})\text{OH}$ . As is shown in Figure 1, a six-center complex is initially formed. If  $\text{D}_2^{18}\text{O}$  were to be mixed with  $\text{CH}_3\text{NO}_2$ , the product would be  $\text{CH}_2\text{N}(\text{O})\text{OD}$ , but the oxygen-18 would remain in the water moiety. Melius's theory also predicts that, as is shown in Figure 2, the interaction of the *aci*- isomer with another molecule of water--again via a six-center complex--would lead to the formation of  $\text{HCNO}$ , with all of the isotopic labelling remaining in the water. Melius's development of the theory for nitramines follows a similar pattern, with six-center intermediates involved in both the initial rearrangement to the *aci*- isomer and the subsequent hydrolysis of this isomer to form molecular fragments. The



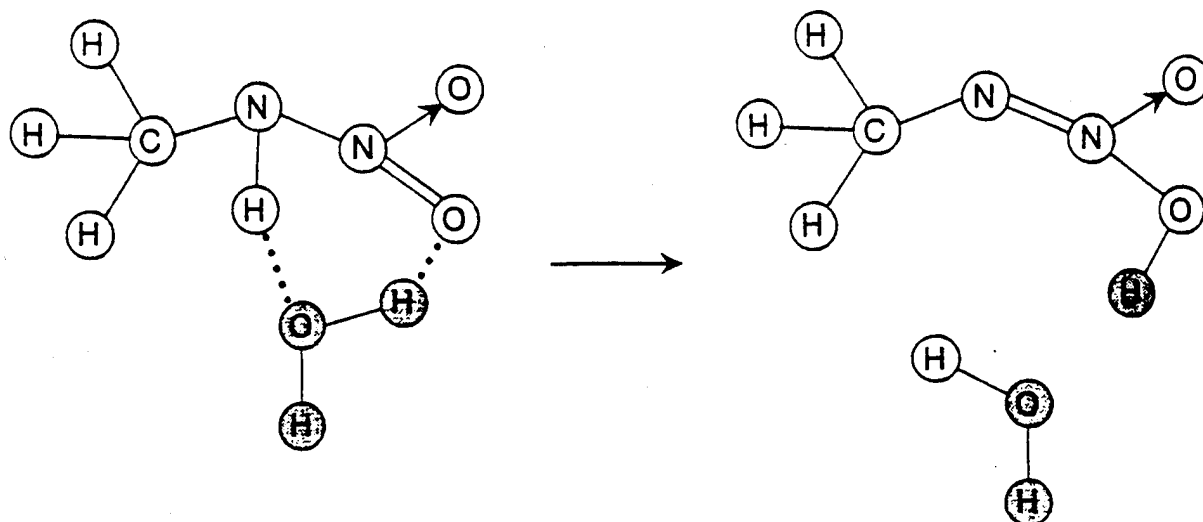
Water-Catalyzed Rearrangement of Nitromethane

Figure 1



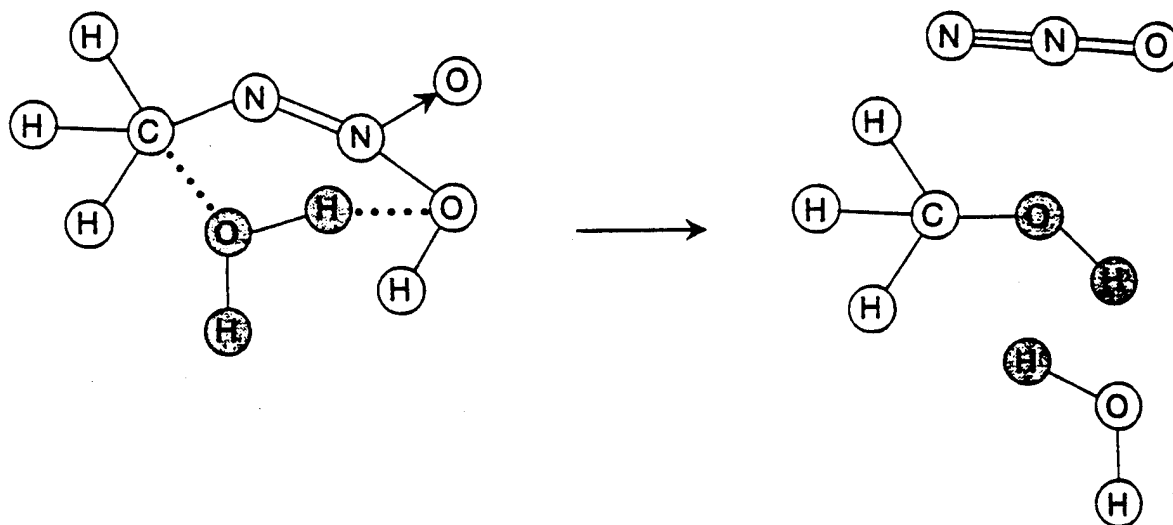
Hydrolysis of aci-Nitromethane

Figure 2



Water-Catalyzed Rearrangement of Monomethylnitramine

Figure 3



Hydrolysis of aci-Monomethylnitramine

Figure 4.

mechanism is shown for monomethylnitramine in Figures 3 and 4. As indicated in Figure 4, the final products are predicted to be nitrous oxide and methanol. Isotopic labelling of the water molecule would transfer to the hydroxyl group of the methanol product, but oxygen-isotopic substitution of the nitrous oxide would not occur.

Melius<sup>2</sup> has extended his theory to predict the modes of decomposition of RDX in both the gas and the condensed phase. At low pressures, catalytic effects are comparatively unimportant. A major mode of decomposition involves initial  $\text{NO}_2$  detachment, followed by the opening of the ring and its fragmentation into one molecule of  $\text{H}_2\text{CN}$  and two of  $\text{CH}_2=\text{NNO}_2$ , hereafter referred to as the monomer, since it is the basic unit of which both RDX and HMX are built. The  $\text{H}_2\text{CN}$ , in turn, fragments into  $\text{HCN} + \text{H}$ , and the monomer into  $\text{H}_2\text{CN} + \text{NO}_2$ . Mowrey and co-workers<sup>3</sup> have published an *ab initio* study of the monomer which provides a more detailed treatment of the transition state than that offered by Melius. They predict that HONO elimination from the monomer, with HCN the other fragment, occurs at a lower energy. In the condensed phase, bimolecular reactions become important. If  $\text{NO}_2$  is detached, it can recombine to form the nitrite, which in turn may eliminate NO.  $\text{NO}_2$  may also abstract an H atom, forming HONO, which reacts with another HONO molecule to form  $\text{H}_2\text{O} + \text{NO} + \text{NO}_2$ . The introduction of  $\text{H}_2\text{O}$  then may facilitate the water-catalyzed decomposition of RDX by a mechanism similar to that for the model compound monomethylnitramine. In the first stage, the ring is broken, and a chain with primary nitramine and hydroxymethyl functional groups is formed. Water then catalyzes the conversion of the primary nitramine into the *aci*- isomer and the subsequent splitting out of  $\text{N}_2\text{O}$ , leaving a hydroxymethyl functional group. The attack of water on the hydroxymethyl end of the chain leads to the detachment of  $\text{H}_2\text{CO}$  and to the



formation of another primary nitramine group. Thus, the water-catalyzed decomposition of RDX or HMX in the condensed phase provides a route to the formation of the often reported end products  $\text{H}_2\text{CO}$  and  $\text{N}_2\text{O}$ .

Ions may also play a significant role in the condensed-phase decomposition of nitroalkanes and nitramines. A series of studies by Engelke and co-workers<sup>4-6</sup> has suggested that the  $\text{CH}_2\text{NO}_2^-$  anion may be an intermediate in the condensed-phase decomposition of nitromethane. Further study of this possible mechanism would be facilitated by the determination of the molecular properties of  $\text{CH}_2\text{NO}_2^-$ . The photoelectron spectrum of this anion has been studied by Metz and co-workers,<sup>7</sup> who were able to determine that it possesses  $\text{C}=\text{N}$  bonding. Their analysis supports the vibrational assignment proposed by Jacox<sup>8,9</sup> as a result of argon-matrix studies of the infrared spectrum of uncharged  $\text{CH}_2\text{NO}_2$ , conducted during earlier periods of Army Research Office support. Spontaneous ion formation, such as dissociation to ionic species in the presence of water, may also occur in other condensed-phase systems, and the resulting ions may contribute to decomposition processes.

A wide variety of uncharged, highly reactive species, many of them free radicals, are expected to be generated in the course of nitramine combustion. Melius<sup>10</sup> has proposed a model for the combustion of RDX that includes 158 elementary reactions involving 38 chemical species. The addition of a binder to the nitramine would further increase the complexity of the combustion process.

The experimental studies reported in the following discussion were performed using the matrix isolation technique, in which a dilute solid solution of the species of interest in a rare gas--usually neon or argon--is prepared and then studied using standard techniques of absorption

spectroscopy. At the temperatures used for these studies, the neon or argon solid is sufficiently rigid that only atoms and electrons can migrate; even small, highly reactive molecules are trapped, and sufficient concentrations of many free radicals and molecular ions can be built up for their direct spectroscopic observation. Because the rare gases are transparent over an extremely wide spectral region, it is possible to study the infrared, near infrared, visible, and ultraviolet absorption spectra of these highly reactive molecules. Infrared spectral studies are especially useful, since the absorptions are very sharp, and small isotopic shifts can be measured, providing a basis for positive identification of the species of interest. The infrared absorptions of a wide variety of transient molecules isolated in solid argon or neon generally lie within 1 % of the corresponding gas-phase band centers.<sup>11</sup> Thus, the chemical bonding properties of the molecule derived from the vibrational frequencies in the matrix compare closely with the corresponding gas-phase properties. Moreover, the vibrational frequencies obtained from the matrix observations can be used to facilitate the development of laser-based diagnostics for free radicals and other highly reactive species in gas-phase reaction systems. Although most chemical reactions are suppressed in the rigid rare-gas solid, cage recombination of fragments resulting from the photodecomposition of a larger molecule trapped in the solid rare gas can occur, providing information on a number of processes which are important at high pressures and in the condensed phase. For example, as a result of an earlier ARO-supported study<sup>12</sup> in this laboratory of the photodecomposition of  $\text{CH}_3\text{NO}_2$  in an argon matrix, it was possible to trace a sequence of several reactions which can occur in the solid state, leading ultimately to the stabilization of  $\text{HNCO} + \text{H}_2\text{O}$ , with the newly discovered species nitrosomethanol as one of the intermediates.

## Scientific Accomplishments

### Infrared Spectrum of H<sub>2</sub>O Trapped in Solid Neon

All of the experiments conducted during the period of this research used neon as the matrix material. Deposits of solid neon are much less optically scattering than are deposits of the heavier rare gases. Moreover, neon experiences minimal interaction with molecules trapped in it. In order to study the spectra of complexes formed by the interaction of water with other substances, it is necessary to have detailed information regarding the contributions of isolated and aggregated water to the spectrum. Although the infrared spectrum of water in the heavier rare gases had been reported by many workers, data were not available for water isolated in a neon matrix. Therefore, infrared and near-infrared spectral observations were conducted<sup>13</sup> between 700 and 8000 cm<sup>-1</sup> on normal and isotopically substituted water trapped in solid neon. As in the heavier rare-gas solids, isolated water molecules can undergo relatively free rotation in solid neon, and transitions arising from the two lowest rotational levels of the water molecule were observed and assigned. The matrix shifts for water isolated in a neon matrix are much smaller than those characteristic of the heavier rare-gas matrices. Absorptions of (H<sub>2</sub>O)<sub>2</sub> were also identified and assigned.

### Interaction of Nitro Compounds with H<sub>2</sub>O

CH<sub>3</sub>NO<sub>2</sub>. A series of measurements was conducted on the infrared spectra of CH<sub>3</sub>NO<sub>2</sub> and of CH<sub>3</sub>NO<sub>2</sub>:H<sub>2</sub>O mixtures isolated in solid neon. Spectral regions in which vibrational fundamentals of CH<sub>3</sub>NO<sub>2</sub> occur are shown in traces (a) of Figures 5 to 7 for a simple Ne:CH<sub>3</sub>NO<sub>2</sub> = 800 deposit. The (b) traces of these three figures show portions of the difference spectrum which was obtained when the spectrum of the (a) traces was subtracted from that

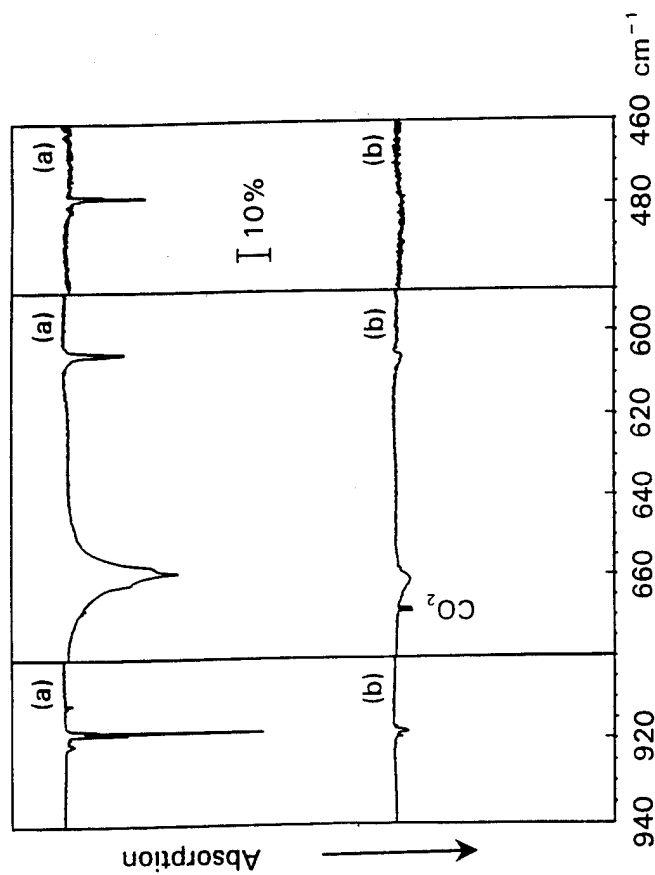


Figure 5

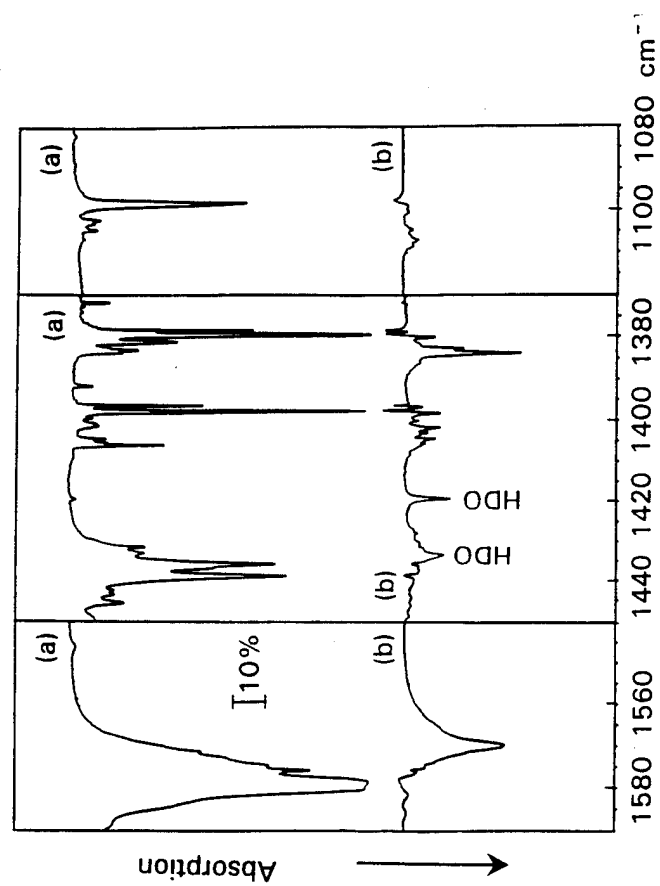


Figure 6

(a)  $\text{Ne}:\text{CH}_3\text{NO}_2 = 800$

(b)  $[\text{Ne}:\text{CH}_3\text{NO}_2:\text{H}_2\text{O} = 800] - [\text{Ne}:\text{CH}_3\text{NO}_2 = 800]$

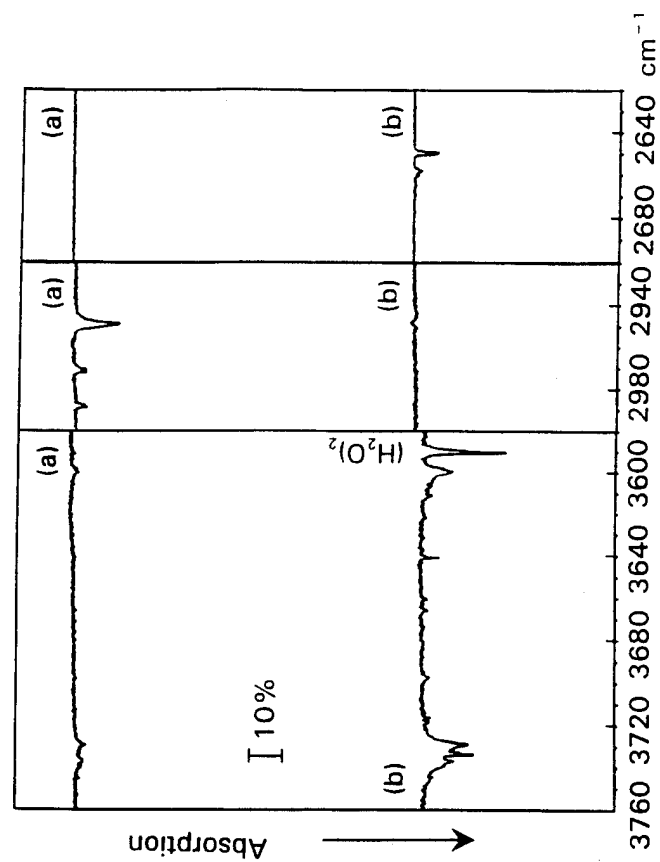


Figure 7

**TABLE I: Comparison of the Absorptions<sup>a</sup> (cm<sup>-1</sup>) of CH<sub>3</sub>NO<sub>2</sub> and of the CH<sub>3</sub>NO<sub>2</sub> Moiety in CH<sub>3</sub>NO<sub>2</sub>·H<sub>2</sub>O Trapped in Solid Neon**

| CH <sub>3</sub> NO <sub>2</sub> | CH <sub>3</sub> NO <sub>2</sub> ·H <sub>2</sub> O | Assignment                |
|---------------------------------|---|---------------------------|
| 477.6                           |   | NO <sub>2</sub> rock      |
| 604.5                           | 605.5   | NO <sub>2</sub> rock      |
| 658.8                           | 660.5   | NO <sub>2</sub> scissors  |
| 917.6                           | 917.8   | C-N stretch               |
| 1098.0                          | 1106.8  | CH <sub>3</sub> rock      |
| 1379.3                          | 1383.7  | NO <sub>2</sub> s-stretch |
| 1397.6                          | 1401.6  | CH <sub>3</sub> deform.   |
| 1435.5                          |   | CH <sub>3</sub> deform.   |
| 1438.6                          |   |                           |
| 1578.6                          | 1569.7  | NO <sub>2</sub> a-stretch |
| 2948.6                          |   | CH <sub>3</sub> stretch   |

<sup>a</sup> ±0.2 cm<sup>-1</sup>.

obtained when the same amount of  $\text{CH}_3\text{NO}_2$  present in a  $\text{Ne}:\text{CH}_3\text{NO}_2:\text{H}_2\text{O} = 800:1:1$  mixture was deposited. The positions of the absorption maxima for isolated  $\text{CH}_3\text{NO}_2$ , obtained for the (a) traces, are compared with those for the maxima in the difference spectrum, which, except for the absorptions of the added  $\text{H}_2\text{O}$  (omitted from Table I), correspond to infrared absorptions of the interaction product. The vibrational assignment for  $\text{CH}_3\text{NO}_2$  proposed by Wilson<sup>14</sup> is included in Table I. The most prominent new absorptions in the difference spectrum are near  $\text{CH}_3\text{NO}_2$  bands that arise primarily from vibrations of the  $\text{NO}_2$  group. This is particularly evident in comparing the difference spectra in the  $1370\text{--}1410\text{ cm}^{-1}$  spectral region with that of  $\text{CH}_3\text{NO}_2$ , which has two transitions of approximately equal intensity in that region. The peak at  $1379\text{ cm}^{-1}$  possesses predominantly  $\text{NO}_2$  symmetric stretching character and can be correlated with the well defined peak near  $1384\text{ cm}^{-1}$  in the difference spectrum. On the other hand, the  $1398\text{ cm}^{-1}$  peak, contributed by a  $\text{CH}_3$  deformation vibration, does not have a prominent counterpart in the difference spectrum. The spectral shifts are small, consistent with the assignment of the absorptions (other than those of excess water) in the difference spectrum to a weakly bound complex of  $\text{CH}_3\text{NO}_2$  with  $\text{H}_2\text{O}$ . The absorptions of the  $\text{H}_2\text{O}$  moiety in the complex were not definitively identified. An OH-stretching absorption may underlie the broad absorption of aggregated water near  $3730\text{ cm}^{-1}$ , or may contribute the rather broad peak near  $3600\text{ cm}^{-1}$ . Although nitrosomethanol,  $\text{CH}_2(\text{NO})\text{OH}$ , has prominent infrared absorptions<sup>12,15</sup> near those of the complex, an alternate assignment to that product was excluded by the poor correspondence of the difference spectrum with the spectrum of nitrosomethanol, produced by unfiltered mercury-arc irradiation of a  $\text{Ne}:\text{CH}_3\text{NO}_2$  deposit. The polarity of the  $\text{NO}_2$  group and the relative prominence of its vibrational absorptions in the difference spectrum suggest that the

$\text{H}_2\text{O}$  is complexed to that part of the  $\text{CH}_3\text{NO}_2$  molecule, consistent with the microwave structure obtained by Lovas and co-workers.<sup>16</sup> No new absorptions in the  $\text{Ne}:\text{CH}_3\text{NO}_2:\text{H}_2\text{O}$  deposits could be attributed to a rearrangement or decomposition product.

When  $\text{Ne}:\text{CH}_3\text{NO}_2$  deposits were exposed to the unfiltered radiation of a medium-pressure mercury arc, the results were similar to those previously reported<sup>12</sup> for  $\text{Ar}:\text{CH}_3\text{NO}_2$  samples. The earlier proposal that HCNO is a photodegradation product were confirmed. After 5 min of unfiltered mercury-arc irradiation, sharp peaks were detected within a few  $\text{cm}^{-1}$  of the positions reported by Bondybey and co-workers<sup>17</sup> for the three stretching fundamentals of HCNO in a neon matrix. The small frequency differences can be attributed to the presence of  $\text{H}_2\text{O}$ , formed in a site adjacent to HCNO in the neon matrix.

**$\text{CH}_3\text{NHNO}_2$ .** Samples of  $\text{CH}_3\text{NHNO}_2$  in a 300- to 500-fold excess of neon were prepared and deposited using a sampling system which was described in an earlier report.<sup>18</sup> The infrared spectra of such deposits always included trace absorptions of  $\text{N}_2\text{O}$  and  $\text{CH}_3\text{OH}$ . The prominence of the absorptions of these two impurities could be minimized by extensive pumping on the solid  $\text{CH}_3\text{NHNO}_2$  before introducing neon into the system. The apparent vapor pressure of the deposit immediately after this extensive pumping was near 13.3 Pa (0.1 Torr). As is shown in Figures 8 and 9, when a thoroughly outgassed  $\text{CH}_3\text{NHNO}_2$  sample was allowed to stand for approximately 16 hours and its vapors were then mixed with neon and deposited, new absorptions appeared near those characteristic of freshly purified  $\text{CH}_3\text{NHNO}_2$ , suggesting the formation of a weakly bound complex. Because the system was leak-tight,  $\text{H}_2\text{O}$ , the principal species remaining in a vacuum system pumped to a low pressure, is a likely participant in this complex. Support for the hypothesis that a complex of  $\text{H}_2\text{O}$  with  $\text{CH}_3\text{NHNO}_2$  is formed results

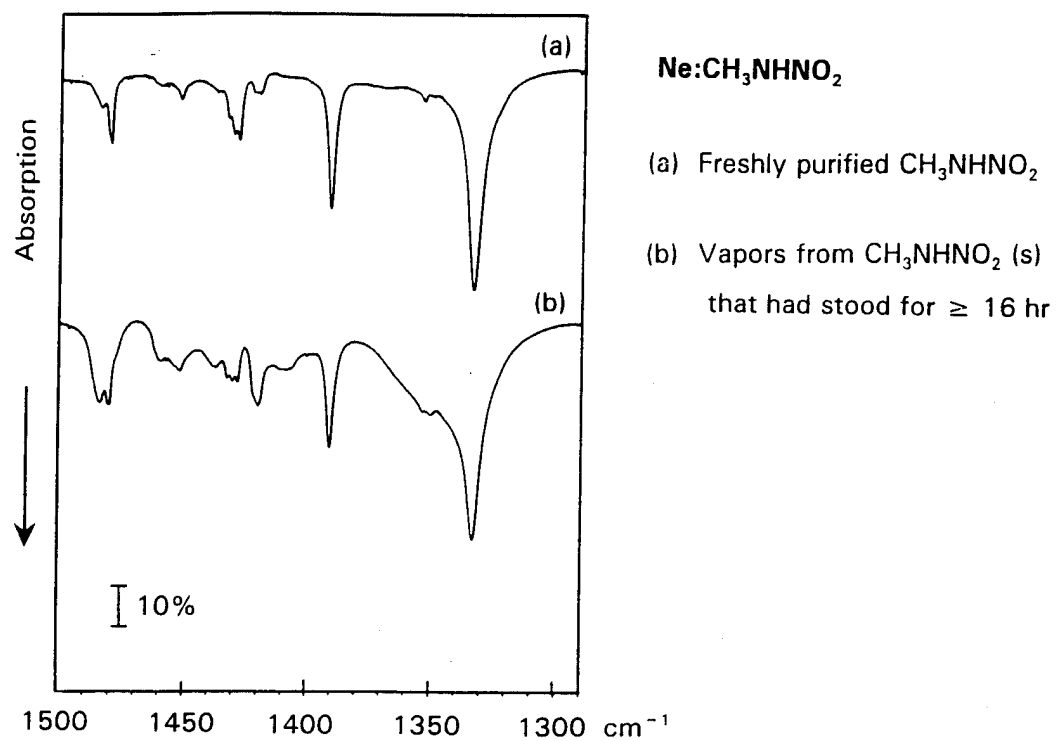


Figure 8

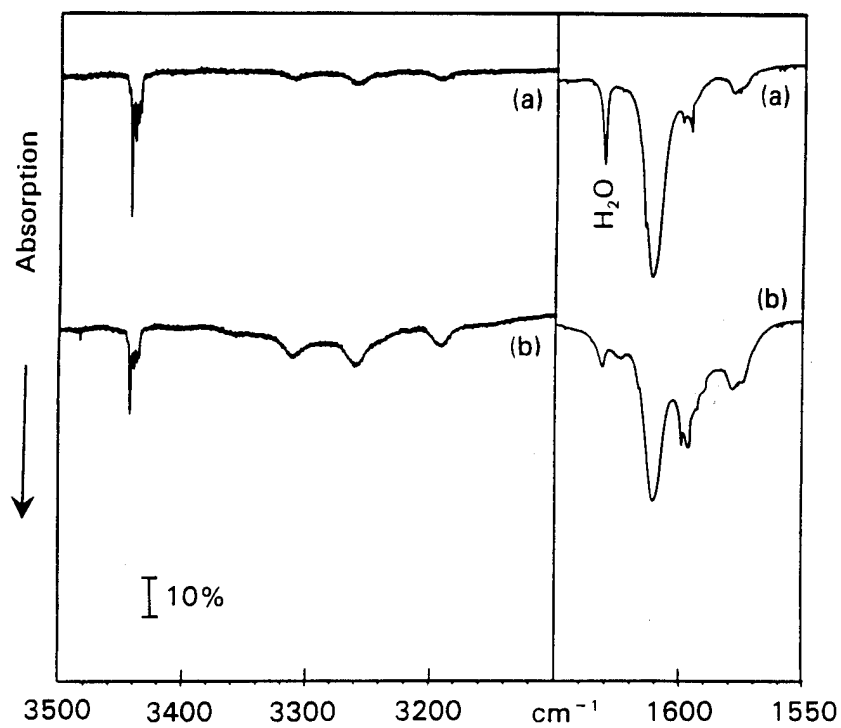
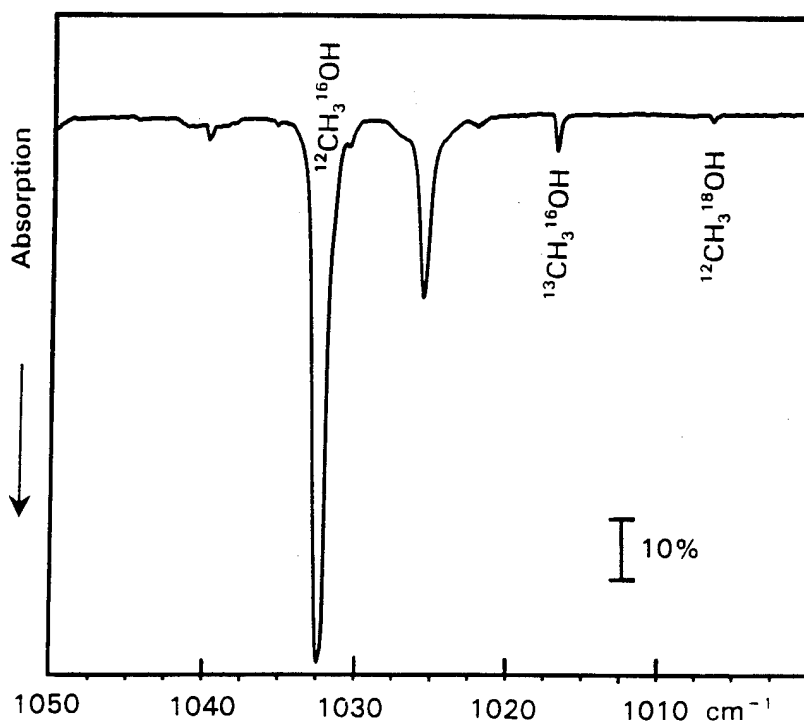
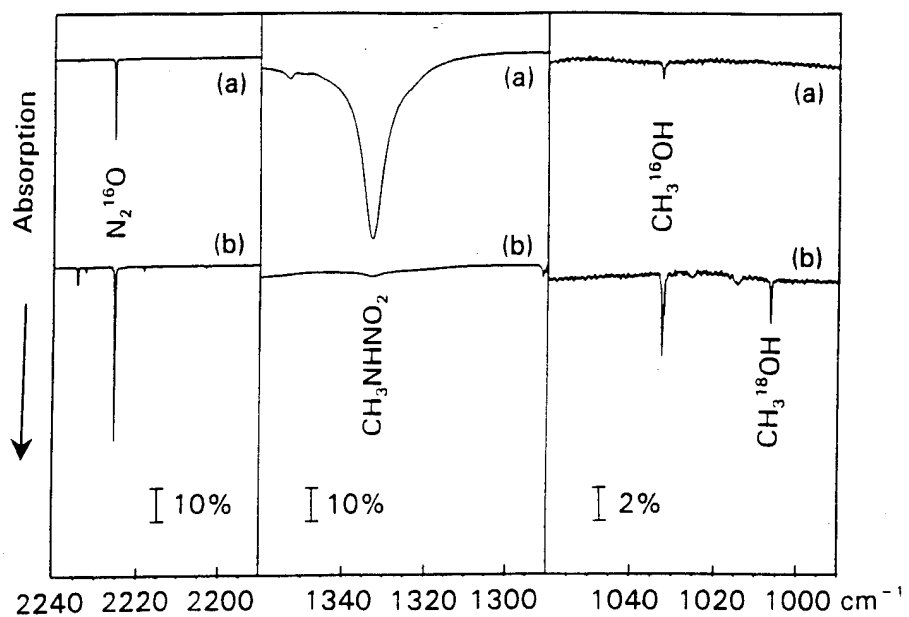


Figure 9



from examination of the absorption pattern near  $1600\text{ cm}^{-1}$ , shown in Figure 9. In trace (b), there is a reduced contribution from the  $1631\text{-cm}^{-1}$  R(0) transition of water rotating in the neon matrix and an enhanced contribution from nonrotating  $\text{H}_2\text{O}$ , near  $1595\text{ cm}^{-1}$ . These changes are characteristic of weak complexes of  $\text{H}_2\text{O}$  with other molecules. The  $\text{NO}_2$  molecule trapped in solid neon has a very strong, sharp absorption at  $1613\text{ cm}^{-1}$ . There is very little evidence for  $\text{NO}_2$  in either trace of Figure 9. The most prominent absorption near  $1610\text{ cm}^{-1}$  is a  $\text{NO}_2$  stretching fundamental of  $\text{CH}_3\text{NHNO}_2$ . The enhancement of its lower frequency satellite near  $1570\text{ cm}^{-1}$  in trace (b) suggests that this band may be contributed by the shifted  $\text{NO}_2$  stretching fundamental of the water complex. The three broad absorptions between  $3180$  and  $3320\text{ cm}^{-1}$  are weak in trace (a) of Figure 9 but more prominent in trace (b), in which the intensity of the structured NH-stretching absorption of  $\text{CH}_3\text{NHNO}_2$  near  $3440\text{ cm}^{-1}$  is reduced. These three broad absorptions may arise from the interaction of  $\text{H}_2\text{O}$  with the NH bond of  $\text{CH}_3\text{NHNO}_2$ , as postulated by Melius<sup>1,2</sup> and illustrated in Figure 3.

Other experiments were designed to test the interaction between  $\text{CH}_3\text{NHNO}_2$  and  $\text{H}_2^{18}\text{O}$ . The results of these studies are illustrated in Figure 10. The spectrum of a deposit prepared using  $\text{CH}_3\text{NHNO}_2$  immediately after purification by extensive pumping, illustrated in Figure 10(a), included the strongest  $\text{CH}_3\text{NHNO}_2$  absorption, near  $1340\text{ cm}^{-1}$ , weaker  $\text{CH}_3\text{NHNO}_2$  absorptions in other spectral regions, and sharp, relatively weak absorptions of  $\text{CH}_3^{16}\text{OH}$  and  $\text{N}_2^{16}\text{O}$ . However, when the solid  $\text{CH}_3\text{NHNO}_2$  was exposed to a small pressure of  $\text{H}_2^{18}\text{O}$  for 42 hours, the residual  $\text{H}_2\text{O}$  vapor was pumped away, and a deposit of size similar to that in the experiment of Figure 10(a) was prepared using the vapors over the  $\text{CH}_3\text{NHNO}_2$  after a modest amount of additional pumping, the resulting spectrum, shown in Figure 10(b), was quite



different. Almost no  $\text{CH}_3\text{NHNO}_2$  was present, and the absorptions of nitrous oxide and methanol, the predominant contributors to the spectrum, were considerably more intense. Although approximately 40% of the methanol was the  $\text{CH}_3^{18}\text{OH}$  isotopic species, there was no evidence for the inclusion of oxygen-18 in the  $\text{N}_2\text{O}$ .

These results are consistent with the mechanism proposed by Melius<sup>1,2</sup> and illustrated in Figures 3 and 4. However, it is conceivable that the inclusion of oxygen-18 in the methanol might have resulted from isotopic exchange between the methanol decomposition product and  $\text{H}_2^{18}\text{O}$ . To check on that possibility, a  $\text{H}_2^{18}\text{O}:\text{CH}_3^{16}\text{OH} = 4:1$  mixture was prepared, condensed into a small volume, held in the liquid phase for 45 hours, vaporized, mixed with a large excess of neon, and deposited on the cryogenic surface. As is shown in Figure 11, the spectrum included an extremely prominent absorption of  $^{12}\text{CH}_3^{16}\text{OH}$  near  $1032\text{ cm}^{-1}$ . The intensities of the corresponding absorptions of  $^{13}\text{CH}_3^{16}\text{OH}$  and  $^{12}\text{CH}_3^{18}\text{OH}$  were approximately those expected on the basis of the natural abundances of carbon-13 and oxygen-18 in the methanol. It was concluded that the oxygen-isotopic exchange observed when  $\text{CH}_3\text{NHNO}_2$  is allowed to stand with  $\text{H}_2^{18}\text{O}$  strongly supports the water-catalyzed nitramine decomposition mechanism proposed by Melius.

### **Photodecomposition of $\text{CH}_3\text{NHNO}_2$**

A preliminary account of the results of the study of the 254-nm photodecomposition of  $\text{CH}_3\text{NHNO}_2$  was presented in an earlier report.<sup>18</sup> A more detailed study, including observations of the photodecomposition of isotopically substituted monomethylnitramine, has yielded a considerable amount of information regarding this process. Samples of  $^{13}\text{CH}_3\text{NHNO}_2$  and of fully deuterated monomethylnitramine were acquired for this study, but the infrared spectra

indicated that the latter sample had experienced isotopic exchange with  $\text{H}_2\text{O}$ , resulting in the predominance of  $\text{CD}_3\text{NHNO}_2$ . Regions of prominent absorption in the infrared spectra of the unphotolyzed deposits of the three isotopomers of monomethylnitramine isolated in solid neon are compared in Figures 12 to 14, and the absorption frequencies are summarized in Table II. The gas-phase band centers for  $\text{CH}_3\text{NHNO}_2$  and  $\text{CD}_3\text{NHNO}_2$  reported by Dakhis and co-workers<sup>19</sup> are included in Table II. There is good agreement between these band centers and the positions of the neon-matrix absorptions. The strong absorption of the deuterium-enriched sample at  $1581.7\text{ cm}^{-1}$ , shown in Figure 14(c), suggests that some fully deuterated monomethylnitramine is still present, but its concentration was insufficient for definitive identification of the ND-stretching fundamental, whereas the NH-stretching absorption was well developed. The small magnitude of the shifts in the  $774.5$ ,  $1332.6$ , and  $1611.4\text{ cm}^{-1}$  absorptions on carbon-13 substitution is consistent with the assignment of these absorptions to vibrations of the  $\text{NO}_2$  group.

The infrared absorptions of the photodecomposition products of these three monomethylnitramine isotopomers are shown in Figures 15 to 20, and their positions, approximate relative intensities, and behavior on prolonged irradiation are summarized in Table III. In order for photodestruction of monomethylnitramine to occur, radiation of wavelength shorter than  $280\text{ nm}$  is required. Unfiltered mercury-arc radiation completely destroys the monomethylnitramine in only a few minutes. More control over the photodestruction is achieved by using a filter of type 9863 glass, which transmits radiation between approximately  $240$  and  $420\text{ nm}$ . Detailed photodestruction studies were conducted on the carbon-13 and the deuterium-substituted monomethylnitramine samples. Four different groups of products were distinguished by their photodestruction behavior.

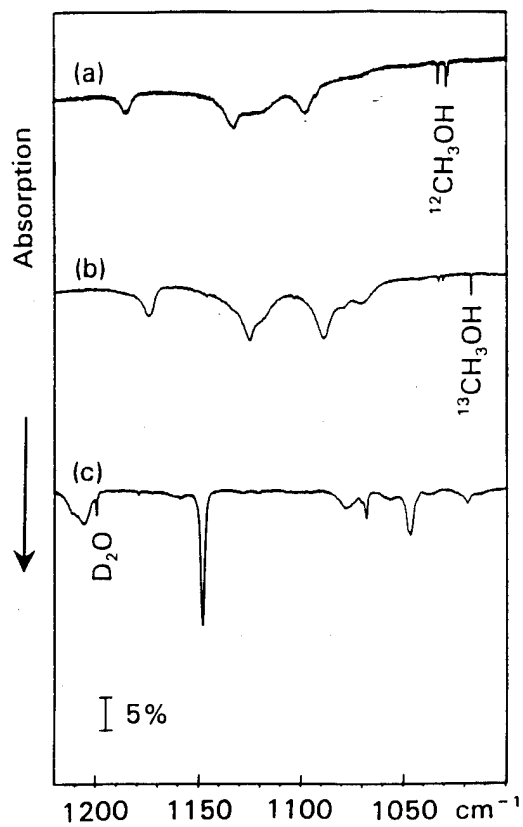


Figure 12

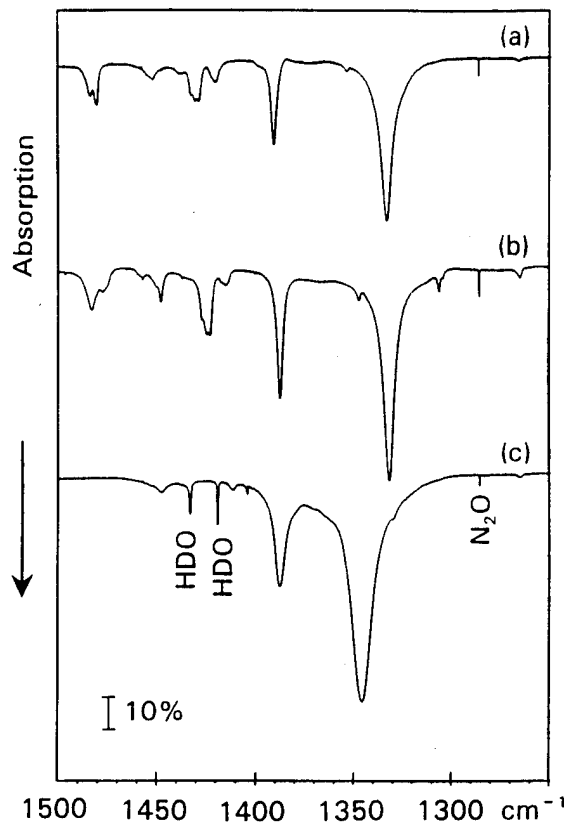
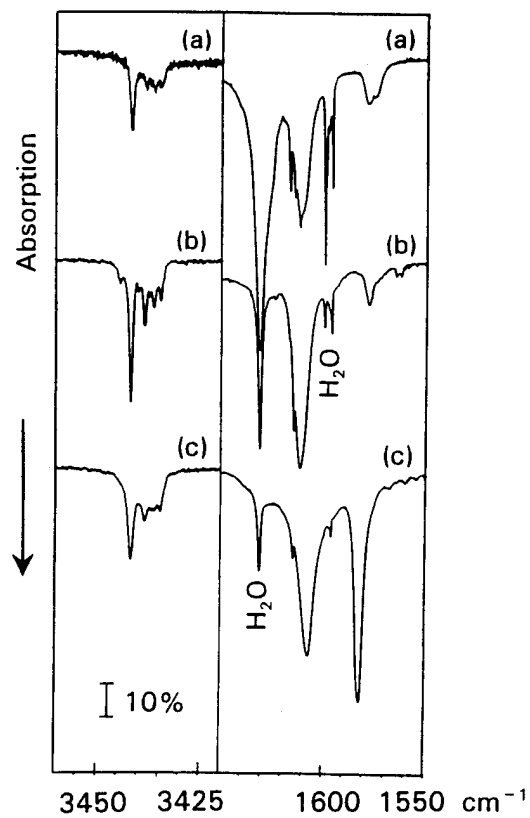


Figure 13



(a)  $\text{Ne}:\text{CH}_3\text{NHNO}_2$

(b)  $\text{Ne}:^{13}\text{CH}_3\text{NHNO}_2$

(c)  $\text{Ne}:\text{CD}_3\text{NHNO}_2$

Initial deposits

Figure 14

**TABLE II: Comparison of the Absorptions<sup>a</sup> (cm<sup>-1</sup>) of Isotopically Substituted Monomethylnitramine Observed in the Gas Phase<sup>b</sup> and in a Neon Matrix**

| $\text{CH}_3\text{NHNO}_2$ |           | $^{13}\text{CH}_3\text{NHNO}_2$ |                    | $\text{CD}_3\text{NHNO}_2$ |  |
|----------------------------|-----------|---------------------------------|--------------------|----------------------------|--|
| gas                        | Ne Matrix | Ne Matrix                       | gas                | Ne Matrix                  |  |
| 595                        |           | 573.3wm                         | 583                | 560.2wm                    |  |
| 727                        |           | 731.2wm,br                      | 695                | 692.0wm,br                 |  |
| 772                        | 774.5wm   | 774.0wm                         | 773                | 770.2m                     |  |
| 928                        |           | 925.0w,br                       | 850                | 850.2s                     |  |
| 1092                       |           |                                 | 1141               | 1147.7s                    |  |
| 1097 <sup>bc</sup>         | 1096.8wm  | 1088.5wm,br                     | 888                | 889.9m,br                  |  |
| 1177 <sup>bc</sup>         | 1132.0wm  | 1124.6wm,br                     | 990                | 958.0m                     |  |
| 1332                       | 1332.6vs  | 1331.6vs                        | 1340               | 1345.9vs                   |  |
| 1394                       | 1390.2s   | 1387.4s                         | 1386               | 1384.3s                    |  |
|                            | 1427.8wm  | 1422.9m                         |                    |                            |  |
|                            | 1429.8m   | 1424.5m                         |                    |                            |  |
| 1434 <sup>bc</sup>         | 1432.1sh  | 1426.7sh                        | 1034 <sup>bc</sup> |                            |  |
| 1454 <sup>bc</sup>         |           | 1447.7wm                        | 1060 <sup>bc</sup> | 1046.2wm                   |  |
| 1470 <sup>bc</sup>         | 1479.8m   | 1477.1sh                        | 1079 <sup>bc</sup> | 1077.2w,br                 |  |
|                            | 1483.0sh  | 1482.8m                         |                    |                            |  |
|                            | 1575.0wm  |                                 |                    | 1541.9wm                   |  |
|                            | 1578.0wm  | 1577.6wm                        |                    |                            |  |
|                            |           |                                 |                    | 1581.7vs                   |  |
| 1614                       | 1611.4vs  | 1611.2vs                        | 1612               | 1606.8vs                   |  |
|                            |           |                                 | 2114               | 2117.7w,br                 |  |
| 3016                       |           |                                 | 2250               | 2244.9wm                   |  |
| 3438                       | 3441.9ms  | 3441.9s                         | 3437               | 3441.5s                    |  |

<sup>a</sup>  $\pm 0.2 \text{ cm}^{-1}$ . w--weak; m--medium; s--strong; vs--very strong; sh--shoulder; br--broad.

<sup>b</sup> Dakhis, M. I.; Dashevsky, V. G.; Avakyan, V. G., J. Mol. Struct. 13, 339 (1972).

<sup>c</sup> Polycrystalline sample measured at 77 K.

The absorptions in group A were relatively prominent after a brief period of irradiation through the filter, but disappeared on somewhat longer irradiation. The structured absorption between about 1834 and 1837  $\text{cm}^{-1}$  falls in this category. Because it is unshifted for the carbon-13 substituted molecule, it is likely to be contributed by a NO-stretching vibration. It shifts by only about 1  $\text{cm}^{-1}$  on deuterium substitution, suggesting that its carrier is not NO complexed to another photofragment, but a compound in which H (or D) is still present. In the experiments on  $^{13}\text{CH}_3\text{NHNO}_2$ , an absorption at 1689.8  $\text{cm}^{-1}$  also showed group A behavior.

Group B absorptions grew throughout the filtered mercury-arc irradiation, but were readily destroyed by unfiltered mercury-arc irradiation. The group B absorptions near 1778 and 1865  $\text{cm}^{-1}$  could be assigned to the NO-stretching fundamentals of *cis*-(NO)<sub>2</sub>. The assignment of several other group B absorptions will be considered later in the discussion.

Group C absorptions also grew throughout the period of filtered mercury-arc irradiation, but diminished much less readily than the group B absorptions on unfiltered mercury-arc irradiation. The 2834  $\text{cm}^{-1}$  group C absorption is in the spectral region appropriate for a CH stretching vibration, but shifts by only 1  $\text{cm}^{-1}$  for the  $^{13}\text{C}$ -substituted product. The counterpart of this absorption for the deuterium-substituted product may be the weak to moderately intense absorption at 2179.6  $\text{cm}^{-1}$  and/or that at 2184.0  $\text{cm}^{-1}$ . The 1646.9  $\text{cm}^{-1}$  group C absorption of the unsubstituted molecule shows only a small shift on carbon-13 substitution and correlates with the 1633.9  $\text{cm}^{-1}$  group C peak in the studies of the deuterium-substituted sample. The absorption near 869  $\text{cm}^{-1}$  is almost completely unshifted in the isotopic substitution experiments.

The absorptions in group D continue to grow as the group B and C absorptions are destroyed on prolonged unfiltered mercury-arc irradiation. These absorptions are readily

assigned to stable end products. Methane and NO are produced, but the position of the NO absorption is slightly shifted by the interaction of that molecule with another species--quite possibly methane. The absorptions of methanol and nitrous oxide are also present, and have group D photodestruction behavior. In the earlier study,<sup>18</sup> although methanol and nitrous oxide absorptions were present, they were not thought to grow on irradiation of the sample. In the present study, absorptions displaced a few  $\text{cm}^{-1}$  from those of methanol and nitrous oxide isolated in solid neon showed group D photodestruction behavior. These absorptions are probably contributed by weakly bound  $\text{CH}_3\text{OH}\cdots\text{N}_2\text{O}$  complexes, which result when a precursor photodecomposes to form these two products trapped in adjacent sites in the solid.

The calculations by Melius<sup>1,2</sup> suggest that the lowest energy thermal decomposition products of monomethylnitramine are  $\text{CH}_2\text{NH}$  and HONO. However, there is a substantial barrier to the formation of these products. Moreover, the photodecomposition may yield a different set of products. Infrared spectral data for  $\text{CH}_2\text{NH}$  have recently been reviewed.<sup>20</sup> The HCNH deformation vibration of that species contributes a very strong absorption at  $1348\text{ cm}^{-1}$  in argon-matrix experiments, and that absorption is shifted only to  $1344.3\text{ cm}^{-1}$  for the gas-phase molecule. Although there are product absorptions at  $1322.9$  and  $1325.6\text{ cm}^{-1}$  in the  $^{13}\text{C}$ -substitution experiments, no nearby peaks were present in the lower yield study of the photodecomposition of unsubstituted monomethylnitramine. The shift in this fundamental of  $\text{CH}_2\text{NH}$  on carbon-13 substitution was reported<sup>21</sup> to amount to  $7\text{ cm}^{-1}$ , suggesting that, if one of these peaks is contributed by  $^{13}\text{CH}_2\text{NH}$ , the corresponding absorption of  $^{12}\text{CH}_2\text{NH}$  should lie between  $1330$  and  $1333\text{ cm}^{-1}$ , in rather poor agreement with the argon-matrix and gas-phase observations. The torsion vibration of  $\text{CH}_2\text{NH}$  trapped in solid argon contributes a very strong



absorption at  $1123\text{ cm}^{-1}$  which is unshifted on carbon-13 substitution. Although there is a group B peak at  $1119.2\text{ cm}^{-1}$ , it shifts by  $4.5\text{ cm}^{-1}$  for the  $^{13}\text{C}$ -substituted product.  $\text{CH}_2\text{NH}$  photodecomposes at  $254\text{ nm}$  to produce  $\text{HNC}$ , a photolytically stable species which should contribute a prominent group D absorption near  $3600\text{ cm}^{-1}$ . Such an absorption was not detected. Similarly, there is scant evidence for the stabilization of *cis*- or *trans*-HONO, the infrared spectra of which have also recently been reviewed,<sup>20</sup> in these experiments. The closest match is that of the  $869\text{-cm}^{-1}$  group C peak to the prominent  $852\text{-cm}^{-1}$  absorption of *cis*-HONO. Conceivably, HONO may form a weakly bound complex with  $\text{CH}_2\text{NH}$  in the matrix. However, the poor correspondence between the behavior of other group B or C absorptions and that appropriate to  $\text{CH}_2\text{NH}$  suggests that the formation of  $\text{CH}_2\text{NH} + \text{HONO}$  is at most a minor photochemical process in these experiments.

Melius's calculations<sup>1,2</sup> indicate that the threshold for  $\text{NO}_2$  detachment from monomethyl-nitramine should lie near  $210\text{ kJ/mol}$  ( $50\text{ kcal/mol}$ ). Very little  $\text{NO}_2$  was detected at any stage of the present experiments. However, cage recombination could suppress  $\text{NO}_2$  formation and could give rise to  $\text{CH}_3\text{NH}\cdot\text{ONO}$ , which Melius estimated to be stable by  $117\text{ kJ/mol}$  ( $28\text{ kcal/mol}$ ). Possibly this product contributes to the group C absorptions. The behavior of the  $1646.9\text{ cm}^{-1}$  peak is appropriate for its assignment to the end  $\text{N}=\text{O}$  stretching fundamental of a nitrite. The  $\text{N}=\text{O}$  stretching fundamental of *trans*- $\text{CH}_3\text{ONO}$  lies at  $1677\text{ cm}^{-1}$  in the gas phase and at  $1666\text{ cm}^{-1}$  in an argon matrix.<sup>22</sup> The corresponding fundamental of *cis*- $\text{CH}_3\text{ONO}$  lies near  $1620\text{ cm}^{-1}$ . As for methyl nitrite, the other NONO skeletal vibrations of the amine nitrite should lie below about  $900\text{ cm}^{-1}$ . Photodecomposition of the amine nitrite might involve H-atom migration, resulting in the formation of the observed products  $\text{CH}_4$  and  $(\text{NO})_2$ . Although the

pattern and photodestruction behavior of the group C absorptions would be consistent with their assignment to the  $\text{CH}_3\text{NHONO}$ , this identification cannot be regarded as definitive.

Still another possible photochemical process would be H-atom detachment and subsequent diffusion from the site. Melius's calculations indicate that  $\text{NO}_2$  would spontaneously detach, leaving  $\text{CH}_2\text{NH}$  as the other fragment. Arguments suggesting that  $\text{CH}_2\text{NH}$  is not present have already been given.

A closely related process would be H-atom migration, which could result either from intramolecular rearrangement or, in the solid, by cage recombination of the photodetached H atom. The predominance of  $\text{CH}_3\text{OH}$  and  $\text{CH}_4$  as the hydrogen-containing final products suggests that CH-bond breaking is not a major process. Migration of the H atom from the NH bond to an O atom could result in the formation of the *aci*- isomer. The group B absorptions include a peak at  $3554.5\text{ cm}^{-1}$ , in the spectral region characteristic of OH-stretching vibrations. This peak persists on substitution of deuterium in the methyl group, consistent with the occurrence of such a migration. The *aci*- species should possess an  $\text{N}=\text{N}$  absorption, as well as absorptions characteristic of an ONO group. These absorptions should not shift very much on deuterium substitution. The group B absorptions which result from the photodestruction of  $\text{CD}_3\text{NHNO}_2$  include peaks at  $1660.8$ ,  $1440.8$ , and  $1326\text{--}1328\text{ cm}^{-1}$  which may arise from such types of vibration. Moreover, the  $702.1\text{ cm}^{-1}$  absorption behaves appropriately for assignment to a  $\text{NO}_2$  deformation. Mercury-arc irradiation, like water catalysis, could surmount the barrier for the decomposition of the *aci*- isomer into  $\text{CH}_3\text{OH} + \text{N}_2\text{O}$ . When these are formed in the solid, they may interact to give a weakly bound  $\text{CH}_3\text{OH}\cdots\text{N}_2\text{O}$  complex.

Still another possible process would be the photodetachment of  $H_2$ , with  $CH_2NNO_2$  the other product. *Ab initio* calculations of the vibrational fundamentals of that product have recently been reported.<sup>3,23</sup> Calculated absorptions at 1839.0 ( $\nu_3$ ) and 1611.9 ( $\nu_4$ )  $cm^{-1}$  would be expected to arise from coupled vibrations of multiply bonded heavy atoms. Although the correspondence of these two vibrational fundamentals with the positions of the two group A absorptions is quite good, there are several problems with such an assignment. In the *ab initio* calculations,<sup>24</sup> the 1839- $cm^{-1}$  fundamental was found to have predominantly CN-stretching character, implying that it should have a large shift on carbon-13 substitution. The calculated peaks at 1612 and 1220  $cm^{-1}$  were predicted to be predominantly  $NO_2$ -stretching vibrations. The lack of a carbon-13 shift in the position of the 1834-1837  $cm^{-1}$  group A absorption indicates that it is not contributed by a CN-stretching vibration. The 1834-1837  $cm^{-1}$  group A absorption lies within a few  $cm^{-1}$  of the position of a prominent  $N_2O_3$  fundamental, and the absorption near 1690  $cm^{-1}$  lies only 7  $cm^{-1}$  below the most prominent absorption of the ONONO isomer.<sup>25</sup> Such an assignment would have reasonably good agreement with the observed frequencies and with the lack of a carbon-13 shift in the 1834-1837  $cm^{-1}$  absorption, but not with the observation of a small deuterium-isotopic shift in that absorption. Moreover,  $N_2O_3$  was found<sup>25</sup> to be photolytically stable (and, in fact, to grow at the expense of ONONO) on mercury-arc irradiation of the neon-matrix deposit through the same filter which permitted photodestruction of the group A peaks in the present study. It is concluded that data do not suffice for a definitive assignment of the group A absorptions.

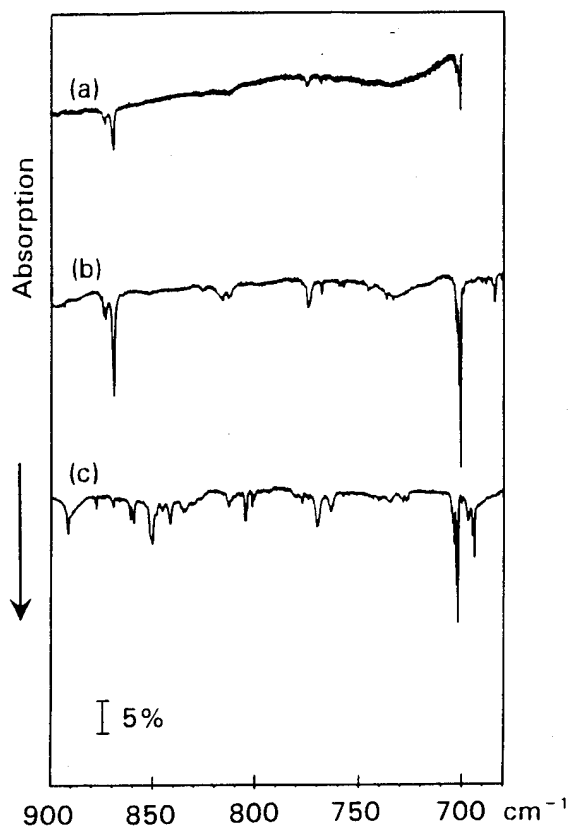


Figure 15

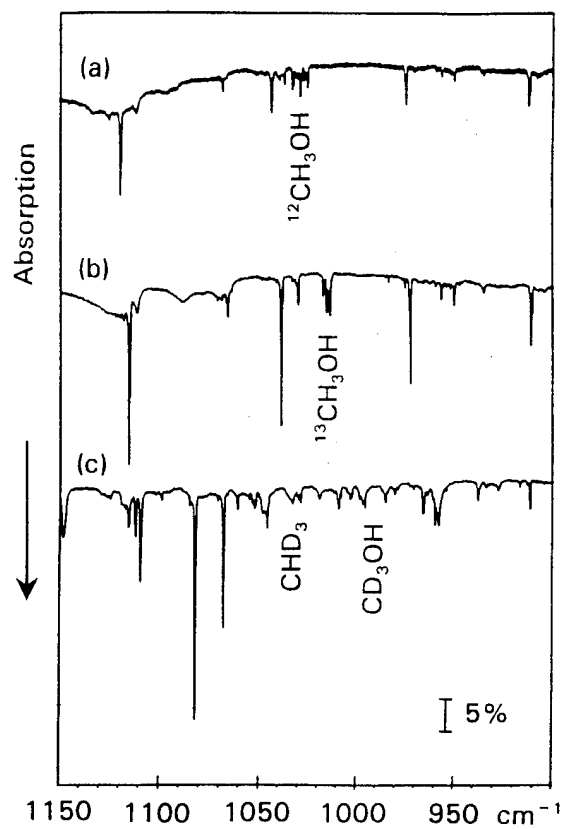


Figure 16

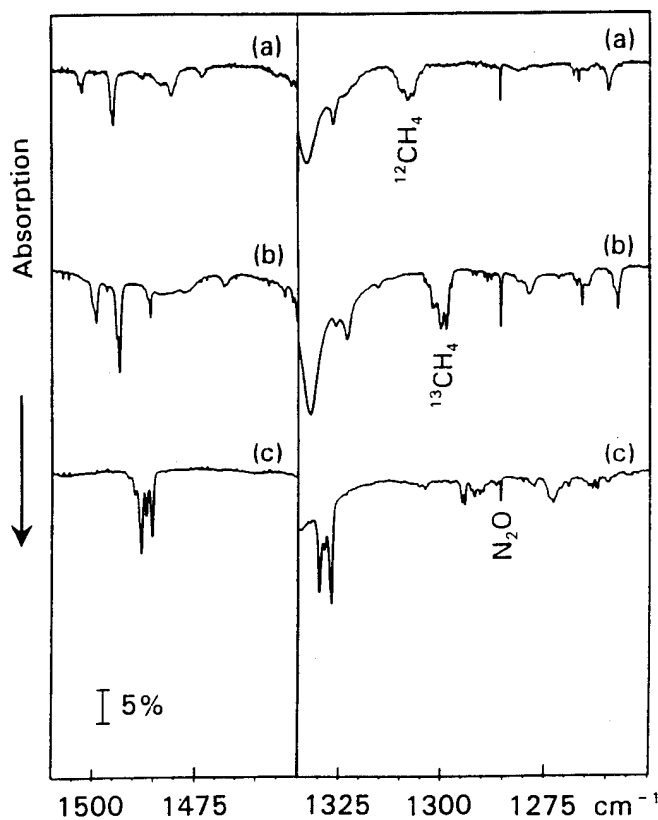


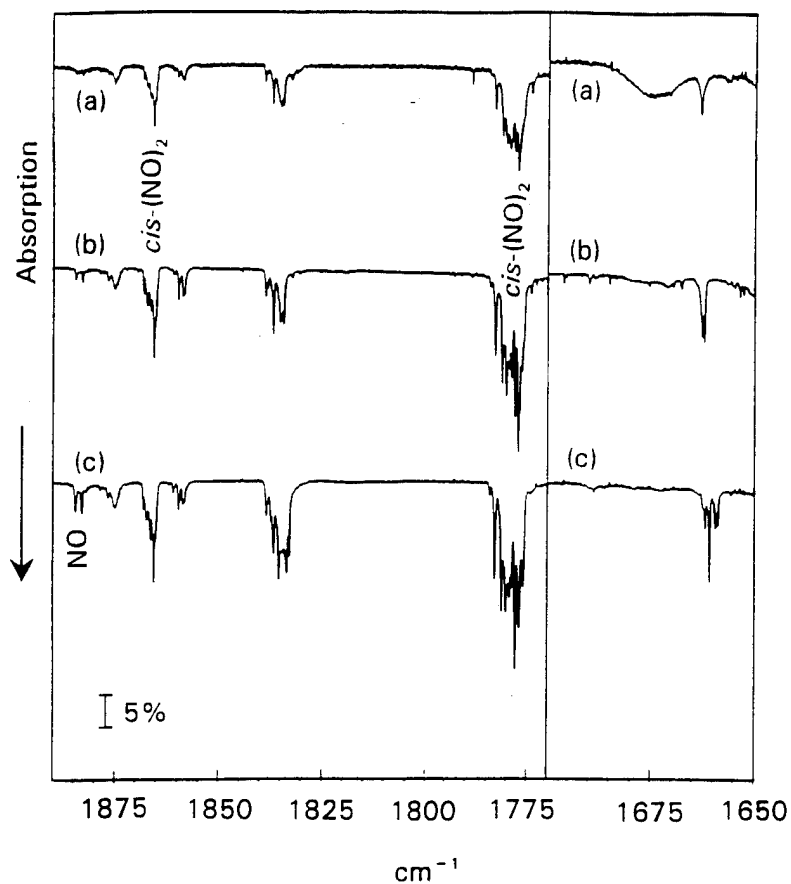
Figure 17

(a) **Ne:CH<sub>3</sub>NHNO<sub>2</sub>**

(b) **Ne:<sup>13</sup>CH<sub>3</sub>NHNO<sub>2</sub>**

(c) **Ne:CD<sub>3</sub>NHNO<sub>2</sub>**

After mercury-arc irradiation,  
240 < λ < 420 nm



(a)  $\text{Ne:CH}_3\text{NHNO}_2$

(b)  $\text{Ne:}^{13}\text{CH}_3\text{NHNO}_2$

(c)  $\text{Ne:CD}_3\text{NHNO}_2$

After mercury-arc irradiation,

$240 < \lambda < 420 \text{ nm}$

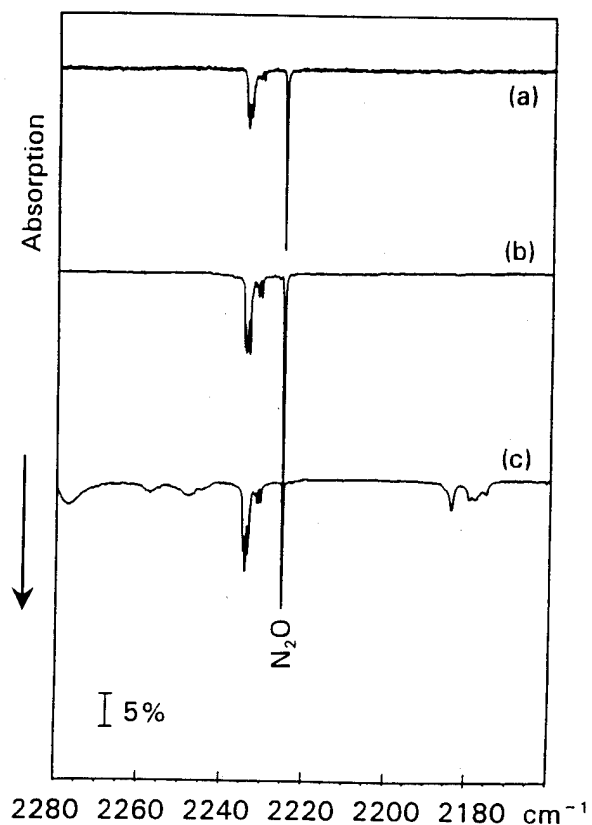


Figure 19

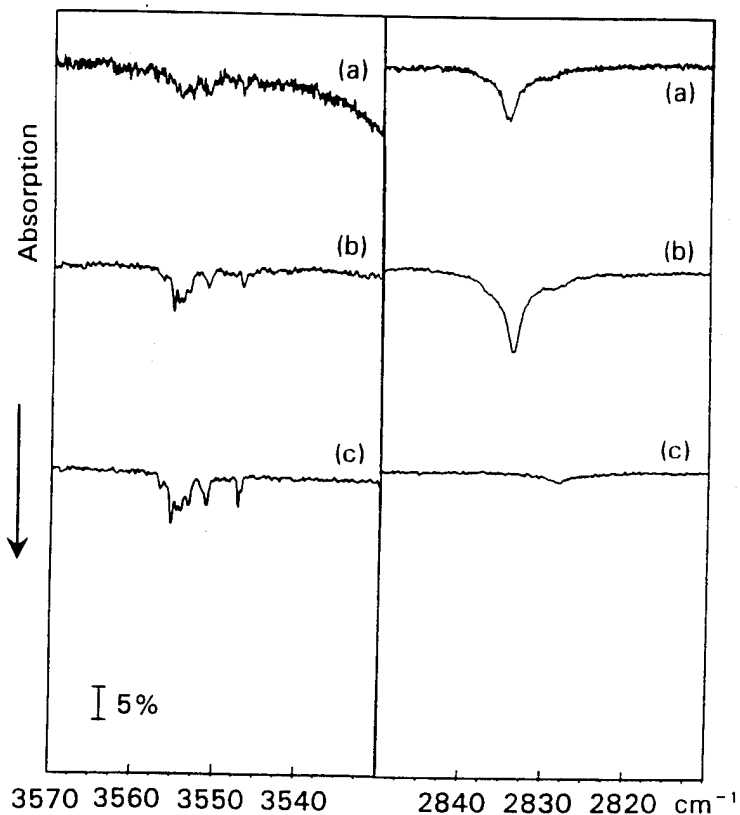


Figure 20

**TABLE III: Photolytic Behavior of Absorptions<sup>a</sup> (cm<sup>-1</sup>) Which Appear on Mercury-Arc Irradiation of Normal and Isotopically Substituted Monomethylnitramine**

| CH <sub>3</sub> NHNO <sub>2</sub> | <sup>13</sup> CH <sub>3</sub> NHNO <sub>2</sub> | CD <sub>3</sub> NHNO <sub>2</sub> | Assignment       |
|-----------------------------------|---|-----------------------------------|------------------|
|                                   | 452.1wm,B                                       |                                   |                  |
|                                   |   | 521.5wm,B                         |                  |
|                                   |   | 524.5m,B                          |                  |
|                                   | 533.6wm,B                                       |                                   |                  |
|                                   | 587.7w,D  |                                   | N <sub>2</sub> O |
|                                   |   | 631.6wm,B                         |                  |
|                                   |   | 640.6m,B                          |                  |
|                                   |   | 660.8w,C                          |                  |
|                                   | 668.6m,B  |                                   |                  |
|                                   |   | 672.2w,C                          |                  |
|                                   | 684.2wm,C                                       |                                   |                  |
|                                   |   | 693.9wm,B                         |                  |
| 700.8m                            | 700.8s,B  | 702.1m,B                          |                  |
|                                   |   | 735.3wm,C                         |                  |
|                                   |   | 777.3wm,C                         |                  |
|                                   |   | 804.7wm,B                         |                  |
|                                   |   | 813.1wm,C                         |                  |
|                                   |   | 841.5wm,C                         |                  |
|                                   |   | 860.0wm,D                         |                  |
| 869.1m                            | 869.2s,C  | 869.5wm,C                         |                  |
| 873.2w                            | 873.2w,C  |                                   |                  |
| 912.0w                            | 911.0m,B  | 911.1wm,B                         |                  |
|                                   |   | 927.2w,C                          |                  |
| 934.4w                            | 934.4w,C  |                                   |                  |
| 949.3wm,-                         | 949.3wm,C                                       |                                   |                  |
|                                   | 951.2vw,D                                       |                                   |                  |
| 955.9wm,-                         | 955.9wm,C                                       |                                   |                  |
|                                   |   | 965.4w,B                          |                  |
| 974.1w                            | 971.7m,B  |                                   |                  |

Table III---Continued

| $\text{CH}_3\text{NHNO}_2$ | $^{13}\text{CH}_3\text{NHNO}_2$ | $\text{CD}_3\text{NHNO}_2$ | Assignment                                 |
|----------------------------|---------------------------------|----------------------------|--|
|                            |                                 | 984.6w,D                   | $\text{CD}_3\text{OH}$                     |
|                            |                                 | 996.6m,D                   | $\text{CD}_3\text{OH}\cdots\text{XY}$      |
|                            |                                 | 1002.6wm,D                 | $\text{CD}_3\text{OH}\cdots\text{XY}$      |
| 1043.1w                    | 1013.1m,D                       |                            | $\text{CH}_3\text{OH}$                     |
|                            | 1015.1m,D                       |                            | $^{13}\text{CH}_3\text{OH}$                |
|                            | 1029.5wm,B                      |                            |  |
|                            |                                 | 1032.6w,br,D               | $\text{CHD}_3$                             |
|                            | 1038.0ms,B                      |                            |  |
| 1067.6w                    | 1065.2wm,D                      | 1067.4m,B                  |  |
|                            |                                 | 1081.6s,B                  |  |
|                            |                                 | 1098.4w,D                  | $\text{CD}_3\text{OH}$                     |
|                            |                                 | 1108.9m,C                  | $\text{CD}_3\text{OH}\cdots\text{XY}$      |
| 1111.0wm                   | 1110.7wm,D                      |                            |  |
|                            |                                 | 1115.0wm,D                 | $\text{CD}_3\text{OH}\cdots\text{XY}$      |
| 1118.7sh                   |                                 |                            |  |
| 1119.2wm                   | 1114.7s,B                       |                            |  |
| 1259.3vw                   | 1257.3wm,B                      |                            |  |
|                            | 1265.9w,B                       |                            |  |
|                            | 1278.8wm,B                      |                            |  |
|                            | 1288.6w,D                       |                            | $\text{N}_2\text{O}$                       |
|                            |                                 | 1290.5wm,D                 | $\text{N}_2\text{O}, \text{CD}_3\text{OH}$ |
|                            | 1291.3w,D                       | 1291.7wm,D                 | $\text{N}_2\text{O}, \text{CD}_3\text{OH}$ |
| 1308.2m                    | 1300.4m,D                       |                            | $\text{CH}_4$                              |
|                            | 1322.9m,B                       | 1326.7m,B                  |  |
|                            | 1325.6wm,B                      | 1328.4m,B                  |  |
|                            | 1399.1w,B                       |                            |  |
| 1415.6wm                   | 1411.6m,B                       | 1415.6w,C                  |  |
|                            |                                 | 1440.8ms,B                 |  |
| 1446.9m,-                  | 1446.8m,C                       |                            |  |
|                            |                                 | 1487.9                     |  |

Table III---Continued

| CH <sub>3</sub> NHNO <sub>2</sub> | <sup>13</sup> CH <sub>3</sub> NHNO <sub>2</sub> | CD <sub>3</sub> NHNO <sub>2</sub> | Assignment                    |
|-----------------------------------|---|-----------------------------------|-------------------------------|
| 1494.6wm                          | 1493.3m,B                                       |                                   |                               |
| 1502.3w                           | 1498.9wm,B                                      |                                   |                               |
|                                   |   | 1516.7w,B                         |                               |
|                                   |   | 1545.5w,D                         |                               |
|                                   |   | 1564.7w,br,C                      |                               |
|                                   | 1614.2wm  |                                   | NO <sub>2</sub>               |
|                                   |   | 1633.9wm,C                        |                               |
|                                   |   | 1637.6wm,A                        |                               |
|                                   |   | 1638.2wm,br,B                     |                               |
| 1646.9wm                          | 1646.6wm,C                                      |                                   |                               |
|                                   |   | 1660.8m,B                         |                               |
|                                   | 1661.9m,B                                       |                                   |                               |
|                                   | 1689.8wm,A                                      |                                   |                               |
| 1777.1m,B                         | 1777.1ms,B                                      |                                   | <i>cis</i> -(NO) <sub>2</sub> |
| 1777.9m,B                         | 1777.9ms,B                                      | 1777.7ms,B                        | <i>cis</i> -(NO) <sub>2</sub> |
| 1834.5wm,A                        | 1834.6m,B                                       | 1833.3m,A                         |                               |
| 1836.6wm,A                        | 1836.6m,B                                       | 1835.2m,A                         |                               |
|                                   | 1858.6wm,B                                      |                                   |                               |
| 1865.5wm,B                        | 1865.4m,B                                       | 1865.4m,B                         | <i>cis</i> -(NO) <sub>2</sub> |
| 1874.9wm,-                        | 1874.9wm,D                                      | 1875.1m,D                         | NO··XY                        |
|                                   |   | 2179.6wm,C                        |                               |
|                                   |   | 2184.0wm,C                        |                               |
|                                   | 2225.3m,D                                       | 2225.3m                           | N <sub>2</sub> O              |
| 2234.5m,-                         | 2234.3m,D                                       | 2234.4m,D                         | N <sub>2</sub> O··XY          |
| 2234.9m,-                         | 2235.0m,D                                       | 2234.9sh,D                        | N <sub>2</sub> O··XY          |
|                                   |   | 2277.1wm,C                        |                               |
| 2834.8m,-                         | 2833.8m,C                                       | 2828.1w,C                         |                               |
|                                   | 3009wm,br,D                                     |                                   |                               |
|                                   | 3117w,br,C                                      |                                   |                               |
|                                   | 3184.2vw,D                                      |                                   |                               |



**Table III---Continued**

| $\text{CH}_3\text{NHNO}_2$ | $^{13}\text{CH}_3\text{NHNO}_2$ | $\text{CD}_3\text{NHNO}_2$ | Assignment |
|----------------------------|---------------------------------|----------------------------|------------|
|                            | 3554.5m,B                       | 3553.2wm,B                 |            |

<sup>a</sup>  $\pm 0.2 \text{ cm}^{-1}$ . vw--very weak; w--weak; m--medium; s--strong; sh--shoulder; br--broad.

- indicates that peak is comparatively weak during irradiation,  $240 < \lambda < 420 \text{ nm}$ .

A--grow in the early stages of mercury-arc irradiation,  $240 < \lambda < 420 \text{ nm}$ , then diminish.

B--grow throughout mercury-arc irradiation,  $240 < \lambda < 420 \text{ nm}$ , readily destroyed on unfiltered mercury-arc irradiation.

C--grow throughout mercury-arc irradiation,  $240 < \lambda < 420 \text{ nm}$ , diminish slowly on unfiltered mercury-arc irradiation.

D--continue to grow on prolonged unfiltered mercury-arc irradiation.

## Other Studies

**Interaction Between  $\text{H}_2\text{O}$  and  $\text{H}_2$ .** In the course of experiments in which a dilute  $\text{Ne}:\text{H}_2$  mixture was passed through the microwave discharge to provide an H-atom source, it was noted that, as is shown in trace (b) of Figure 21, a new absorption consistently appeared approximately  $10\text{ cm}^{-1}$  below the most prominent  $\nu_3$  absorption of water rotating in the neon matrix, at  $3783\text{ cm}^{-1}$ . In the region of the  $\text{H}_2\text{O}$  bending fundamental, the absorption of nonrotating water near  $1595\text{ cm}^{-1}$  was also greatly enhanced. Moreover, as is shown in trace (b) of Figure 22, a new absorption appears near the position of the vibrational fundamental of  $\text{H}_2$ , which is normally infrared-inactive. If  $\text{D}_2$ , instead of  $\text{H}_2$ , is introduced in the system, this latter absorption is shifted to approximately  $2990\text{ cm}^{-1}$ , near the position of the vibrational fundamental of  $\text{D}_2$ , but the perturbed  $\text{H}_2\text{O}$  absorptions change only slightly. This behavior has been interpreted as arising from the formation of a weakly bonded  $\text{H}_2\text{O}\cdots\text{H}_2$  complex.

**H +  $\text{CH}_3\text{NO}_2$  Reaction.** This same discharge H-atom source was used in experiments to study the infrared spectrum which results from the reaction of H atoms with  $\text{CH}_3\text{NO}_2$ . Since no products were detected, it was concluded that the previously reported barrier to this reaction was sufficiently high to prevent its occurrence under the sampling conditions of these experiments.

**Infrared and Near Infrared Spectra of HCC and DCC.** One of the most important free radicals in hydrocarbon decomposition and combustion is HCC. When a binder is added to the nitramine, HCC will also participate in the nitramine combustion mechanism. The first excited electronic state of HCC, of  $^2\Pi$  symmetry, has its origin near  $3700\text{ cm}^{-1}$ . Because the ground-state bending fundamental of HCC lies at the exceptionally low frequency of  $371\text{ cm}^{-1}$ ,

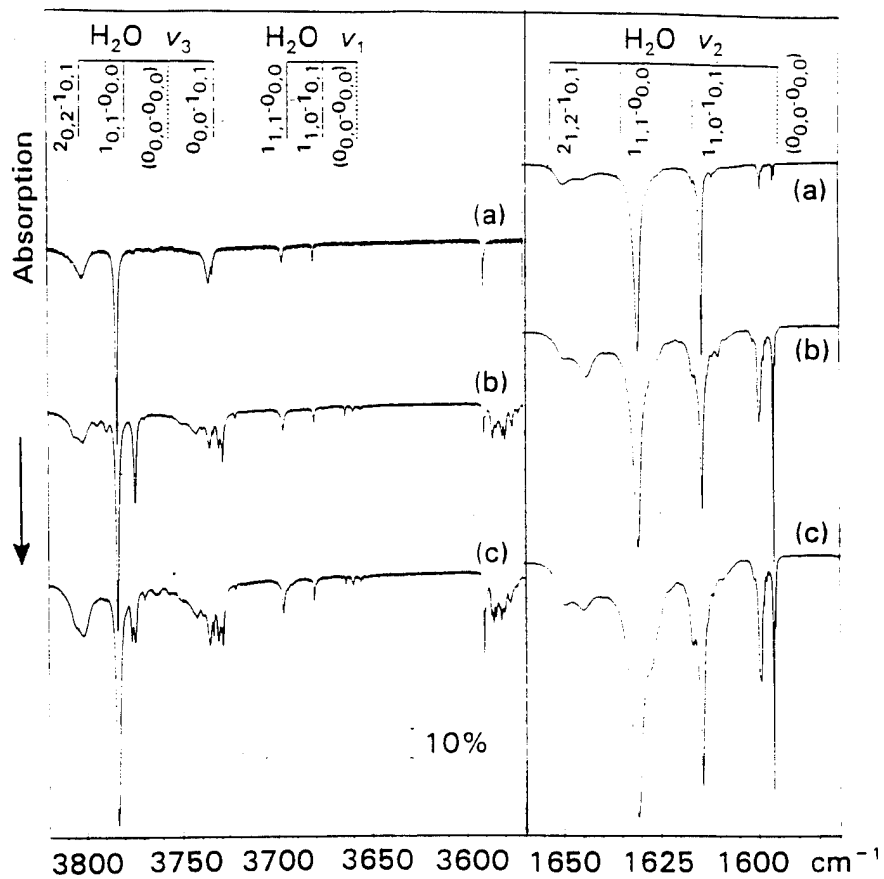


Figure 21

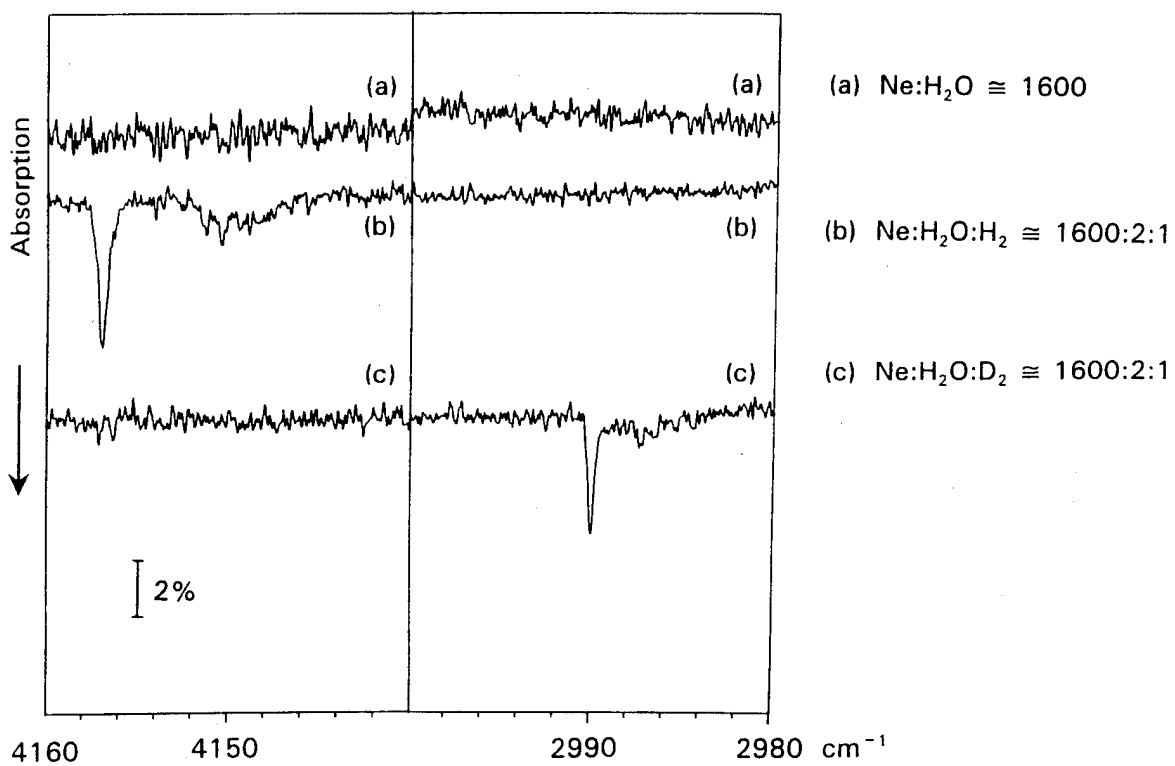


Figure 22

there are many overtones and combination bands of  $^2\Pi$  symmetry near and above  $3700\text{ cm}^{-1}$ . These ground-state energy levels interact strongly with levels of the  $\tilde{A}\ ^2\Pi$  electronic state which have  $\Pi$  vibronic symmetry. Ground-state energy levels of  $\Sigma^+$  vibronic symmetry also interact with  $\tilde{A}$  state energy levels which have  $\Sigma^+$  vibronic symmetry. There results a very complicated spectrum, in which levels of the ground and excited electronic states are strongly mixed. Only a few of the possible transitions have been detected and analyzed in the gas phase. The matrix isolation spectra includes approximately 60 bands between  $3500$  and  $9000\text{ cm}^{-1}$ , all of which must arise from the ground electronic and vibrational state of HCC. Where gas-phase measurements are available, the matrix shift is small, suggesting the utility of matrix isolation observations in the search for new gas-phase bands. The determination of carbon-13 isotopic shifts for the HCC bands provides important input to the extremely difficult task of assigning them. A detailed analysis of the infrared and near infrared bands of HCC and of DCC, observed in argon and neon matrices, was conducted, and the results have recently been published.<sup>26</sup>

**Molecular Ions.** A unique capability for studying the infrared spectra of small molecular ions has been developed in this laboratory.<sup>18</sup> During the period covered by this report, infrared spectral data have been obtained for several ionic species which are especially likely to be important in nitramine decomposition systems.

The ubiquity of water suggests that when ionization can occur  $\text{H}_2\text{O}^+$  will be likely to participate in the chemistry of the system. Accordingly, studies of this molecular ion were conducted, and all three vibrational fundamentals of both  $\text{H}_2\text{O}^+$  and  $\text{D}_2\text{O}^+$  were detected and assigned.<sup>27</sup> Changes in the pattern of rotational excitation of the uncharged  $\text{H}_2\text{O}$  absorptions

pattern on the magnitude of the ion field has proved to be a useful indicator of the presence of ions in the neon matrix.

In studies on Ne:NO<sub>2</sub> and Ne:NO:O<sub>2</sub> samples, the very prominent  $\nu_3$  absorptions of both NO<sub>2</sub><sup>+</sup> and NO<sub>2</sub><sup>-</sup>, as well as the  $\nu_1 + \nu_3$  combination bands of both of these species, were detected and assigned.<sup>28</sup> In addition, evidence was obtained for the stabilization of NO<sub>3</sub><sup>-</sup> in sites in the neon lattice in which perturbation by nearby cations is minimal. Under these conditions, the infrared absorption pattern of NO<sub>3</sub><sup>-</sup> should approximate that of the gas-phase species.

Attempts were made to stabilize in a neon matrix the ionic species which result from the photoionization and/or Penning ionization of CH<sub>3</sub>NO<sub>2</sub> by neon atoms excited to the 16.6-16.8 eV range. NO<sub>2</sub> was not observed to be formed under those conditions. The most prominent product absorptions were near 1025 and 1230 cm<sup>-1</sup>. Each of these shifted a few cm<sup>-1</sup> in a study of the spectrum which resulted when a <sup>13</sup>CH<sub>3</sub>NO<sub>2</sub> sample was used. This shift was too small for the absorption near 1025 cm<sup>-1</sup> to be assigned to CH<sub>3</sub>O, which has its CO-stretching absorption in that spectral region. Unfortunately, the CH<sub>3</sub><sup>15</sup>NO<sub>2</sub> sample contained a major impurity. Observations on a new CH<sub>3</sub><sup>15</sup>NO<sub>2</sub> sample are planned, and may be helpful in assigning the observed absorptions, as well as in determining whether NO<sup>+</sup> or NO<sub>2</sub><sup>+</sup>, each of which would be obscured by CO<sub>2</sub> ( $\nu_3$ ) absorption, is present.

### Publications

1. D. Forney, M. E. Jacox, and W. E. Thompson, "The Mid- and Near-Infrared Spectra of Water and Water Dimer Isolated in Solid Neon," J. Mol. Spectrosc. **157**, 479-493 (1993).
2. D. Forney, M. E. Jacox, and W. E. Thompson, "The Vibrational Spectra of Molecular Ions Isolated in Solid Neon. X.  $\text{H}_2\text{O}^+$ ,  $\text{HDO}^+$ , and  $\text{D}_2\text{O}^+$ ," J. Chem. Phys. **98**, 841-849 (1993).
3. D. Forney, W. E. Thompson, and M. E. Jacox, "The Vibrational Spectra of Molecular Ions Isolated in Solid Neon. XI.  $\text{NO}_2^+$ ,  $\text{NO}_2^-$ , and  $\text{NO}_3^-$ ," J. Chem. Phys. **99**, 7393-7403 (1993).
4. D. Forney, M. E. Jacox, and W. E. Thompson, "The Infrared and Near-Infrared Spectra of HCC and DCC Trapped in Solid Neon," J. Mol. Spectrosc. **170**, 178-214 (1995).

Other papers are planned reporting the following results:

- (a) Interaction of nitro compounds with  $\text{H}_2\text{O}$
- (b) Photodecomposition of  $\text{CH}_3\text{NHNO}_2$
- (c) Interaction between  $\text{H}_2\text{O}$  and  $\text{H}_2$

### Participants in ARO Research

Dr. Marilyn E. Jacox, Principal Investigator

Dr. Warren E. Thompson, Guest Researcher

Dr. Daniel Forney, Guest Researcher

## References

1. C. F. Melius, J. Phys. Colloq. C4, **48**, 341 (1987).
2. C. F. Melius, "Thermochemical Modeling: I. Application to Decomposition of Energetic Materials," in *Chemistry and Physics of Energetic Materials*, S. N. Bulusu, Ed., Kluwer Academic Publishers, Dordrecht, The Netherlands, 1990, pp 21-49.
3. R. C. Mowrey, M. Page, G. F. Adams, and B. H. Lengsfeld III, J. Chem. Phys. **93**, 1857 (1990).
4. R. Engelke, W. L. Earl, and C. M. Rohlfiing, J. Chem. Phys. **84**, 142 (1986).
5. R. Engelke, W. L. Earl, and C. M. Rohlfiing, J. Phys. Chem. **90**, 545 (1986).
6. R. Engelke, D. Schiferl, C. B. Storm, and W. L. Earl, J. Phys. Chem. **92**, 6815 (1988).
7. R. B. Metz, D. R. Cyr, and D. M. Neumark, J. Phys. Chem. **95**, 2900 (1991).
8. M. E. Jacox, J. Phys. Chem. **87**, 3126 (1983).
9. M. E. Jacox, J. Phys. Chem. **91**, 5038 (1987).
10. C. F. Melius, "Thermochemical Modeling: II. Application to Ignition and Combustion of Energetic Materials," in *Chemistry and Physics of Energetic Materials*, S. N. Bulusu, Ed., Kluwer Academic Publishers, The Netherlands, 1990, pp. 51-78.
11. M. E. Jacox, Chem. Phys. **189**, 149 (1994).
12. M. E. Jacox, J. Phys. Chem. **88**, 3373 (1984).
13. D. Forney, M. E. Jacox, and W. E. Thompson, J. Mol. Spectrosc. **157**, 479 (1993).
14. T. P. Wilson, J. Chem. Phys. **11**, 361 (1943).
15. R. P. Müller, J. R. Huber, and H. Hollenstein, J. Mol. Spectrosc. **104**, 209 (1984).

16. F. J. Lovas, N. Zobov, G. T. Fraser, and R. D. Suenram, *J. Mol. Spectrosc.* **171**, 189 (1995).
17. V. E. Bondybey, J. H. English, C. W. Mathews, and R. J. Contolini, *J. Mol. Spectrosc.* **92**, 431 (1982).
18. M. E. Jacox, *Spectroscopy of Reaction Intermediates in Nitramine Decomposition and Combustion*, U. S. Army Research Office, Final Report, Proposal 25664-CH (20 June 1991).
19. M. I. Dakhis, V. G. Dashevsky, and V. G. Avakyan, *J. Mol. Struct.* **13**, 339 (1972).
20. M. E. Jacox, *Vibrational and Electronic Energy Levels of Polyatomic Transient Molecules*, Monograph No. 3, *J. Phys. Chem. Ref. Data* (1994).
21. M. E. Jacox and D. E. Milligan, *J. Mol. Spectrosc.* **56**, 333 (1975).
22. F. L. Rook and M. E. Jacox, *J. Mol. Spectrosc.* **93**, 101 (1982).
23. B. M. Rice, G. F. Adams, M. Page, and D. L. Thompson, *J. Phys. Chem.* **99**, 5016 (1995).
24. B. M. Rice, private communication.
25. M. E. Jacox and W. E. Thompson, *J. Chem. Phys.* **93**, 7609 (1990).
26. D. Forney, M. E. Jacox, and W. E. Thompson, *J. Mol. Spectrosc.* **170**, 178 (1995).
27. D. Forney, M. E. Jacox, and W. E. Thompson, *J. Chem. Phys.* **98**, 841 (1993).
28. D. Forney, W. E. Thompson, and M. E. Jacox, *J. Chem. Phys.* **99**, 7393 (1993).